ISSN 1063-7729, Astronomy Reports, 2011, Vol. 55, No. 12, pp. 1096–1104. © Pleiades Publishing, Ltd., 2011.
Original Russian Text © A.G. Gorshkov, A.V. Ipatov, V.K. Konnikova, A. Lähteenmäki, V.V. Mardyshkin, M.G. Mingaliev, E. Nieppola, J. Tammi, A.M. Finkel'shtein, M.A. Kharinov, 2011, published in Astronomicheskii Zhurnal, 2011, Vol. 88, No. 12, pp. 1188–1196.

Rapid Variability of the Radio Flux Density of the Blazar J0721+7120 (S5 0716+714) in 2010

A. G. Gorshkov[1], A. V. Ipatov[2], V. K. Konnikova[1], A. Lähteenmäki[3], V. V. Mardyshkin[2], M. G. Mingaliev[4], E. Nieppola[3], J. Tammi[3], A. M. Finkel'shtein[2], and M. A. Kharinov[2]

[1] *Sternberg Astronomical Institute, Moscow State University, Universitetskii pr. 13, Moscow, 119234 Russia*

[2] *Institute of Applied Astronomy, Russian Academy of Sciences, Zhdanovskaya ul. 8, St. Petersburg, 197110 Russia*

[3] *Metsähovi Radio Observatory, Aalto University, Metsähovintie 114, FIN-02540 Kylmälä, Finland*

[4] *Special Astrophysical Observatory, Russian Academy of Sciences, Nizhnii Arkhyz, Karachai-Cherkessian Republic, 357169 Russia*

Received February 4, 2011; in final form, April 11, 2011

Abstract—Results of a study of the variability of the blazar J0721+7120 carried out on the RATAN-600 based on daily observations from March 5, 2010 to April 30, 2010 at five frequencies from 2.3 to 21.7 GHz are reported. In the same time interval, 13 observing sessions at 37 GHz were carried out on the 14-m radio telescope of the Metsähovi Radio Astronomy Observatory of the Aalto University School of Technology (Finland). From March 19, 2010 to October 20, 2010, 16 daily sessions at 6.2 cm and five sessions at 3.5 cm were conducted on the 32-m radio telescope of the Zelenchukskaya Observatory (Quasar-KVO complex of the Institute of Applied Astronomy, Russian Academy of Sciences). A powerful flare was detected during the observations, with a time scale of approximately 20 days, derived from an analysis of the light curves and the structure and autocorrelation functions. The flare spectrum has been determined. In five sessions on the 32-m Zelenchukskaya telescope at 6.2 cm, intraday variability with time scales 8–16 h was detected; in four sessions, trends with time scales longer than a day were observed. In three sessions at 3.5 cm, intraday variability with a time scale of approximately 5 h was detected.

DOI: 10.1134/S1063772911120043

1. INTRODUCTION

The radio source J0721+7120 belongs to a bright ($S_{5\,\mathrm{GHz}} > 1$ Jy) sample of sources with flat spectra ($\alpha \geq -0.5$, $S_\nu \sim \nu^\alpha$) of the S5 catalog [1]. J0721+7120 is identified with a bright optical object (12^m) with a featureless continuum, and its redshift has not been measured directly. Nilsson et al. [2] reported the detection of a host galaxy with an estimated redshift of $z = 0.31$.

Since the non-thermal component dominates in the optical spectrum, it is natural to suppose that the spectrum is formed by the emission of a jet that is nearly aligned with the line of sight. Based on the time delay in the development of flares, Vol'vach et al. [3] inferred the Lorentz factor $\gamma = 45-50$ and angle to the line of sight $\theta \approx 1/\gamma^2 = 1^\circ-1.5^\circ$.

This jet orientation makes the relative variability amplitude of this object one of the highest among all Active Galactic Nuclei (AGNs), and variability is detected in all wavelength ranges, from radio to gamma rays. The characteristics of the variability with references to original papers were reviewed in our paper [4]. The surprising similarity of the variability characteristics in all wavelength ranges is striking, and testifies to a unified emission mechanism.

The presence of intraday variability (IDV) suggests that the brightness temperatures considerably exceed the inverse-Compton limit during flares. The correlation of IDV on time scales of several days in the optical and radio [5] and the spectrum of this variability [6] indicate an intrinsic origin for the IDV, which requires a Doppler factor $\delta \simeq 20$ [6]. The intraday time scales require anomalously high Doppler factors; therefore, it is also necessary to consider external causes for the IDV.

The aim of our research was to analyze the variability of J0721+7120 in a broad frequency range from 37 to 2.3 GHz on time scales from several hours to tens of days. During 57 days, we conducted daily observations on the RATAN-600 radio

† Deceased.

telescope, 13 observing sessions on the Metsähovi Radio Observatory at 37 GHz, and 21 daily observing sessions on the 32-m Zelenchukskaya telescope of the Institute of Applied Astronomy at 3.5 and 6.2 cm.

2. OBSERVATIONS AND REDUCTION

2.1. RATAN-600

Observations of J0721+7120 were conducted daily on the Southern Sector of the RATAN-600 radio telescope in the lower culmination from March 5 to April 30, 2010, simultaneously at 2.3, 4.85, 7.7, 11.1, and 21.7 GHz. We processed the observations using a software package that enabled us to derive the flux density of an individual observation of the source as well as the average flux density for any interval within a series of observations. The processing was based on optimal filtration of the input data; the technique used is described in detail in [7, 8].

We used J0701+6951, which has a power-law spectrum, as a calibration source, and adopted the flux densities 1175, 628, 426, 314, and 180 mJy at 2.3, 4.85, 7.7, 11.1, and 21.7 GHz, respectively.

2.2. IAA 32-m Radio Telescope

Observations aimed at studies of intraday variability of J0721+7120 were carried out at 3.5 and 6.2 cm on the 32-m radio telescope of the Zelenchukskaya Observatory of the Quasar-KVO complex (Institute of Applied Astronomy, Russian Academy of Sciences).

The observations were conducted in a "smooth scanning" mode in elevation [9]: the antenna tracked the source in azimuth and performed scanning in elevation. The cycle was repeated the number of times required to accumulated the desired quantity of data; N cycles of observations of the reference or target source were called a session. Twenty-one successful daily sessions were conducted from March 19 to September 20, 2010.

We chose the same reference source as in the RATAN-600 observations. The technique used for the observations and processing are described in detail in [10].

2.3. Metsähovi 14-m Radio Telescope

In the time interval of interest for us, 13 observations of J0721+7120 unevenly distributed in time were conducted at 37 GHz at the Metsähovi Radio Observatory of the Aalto University School of Technology (Finland). A standard ON–ON technique was employed, in which antenna temperatures were recorded with the radio telescope pointing alternately to one of the two beam positions. The antenna temperatures corrected for absorption in the Earth's atmosphere were recalculated to flux densities using observations of a calibration source, taking into account the dependence of the effective area of the radio telescope on the elevation.

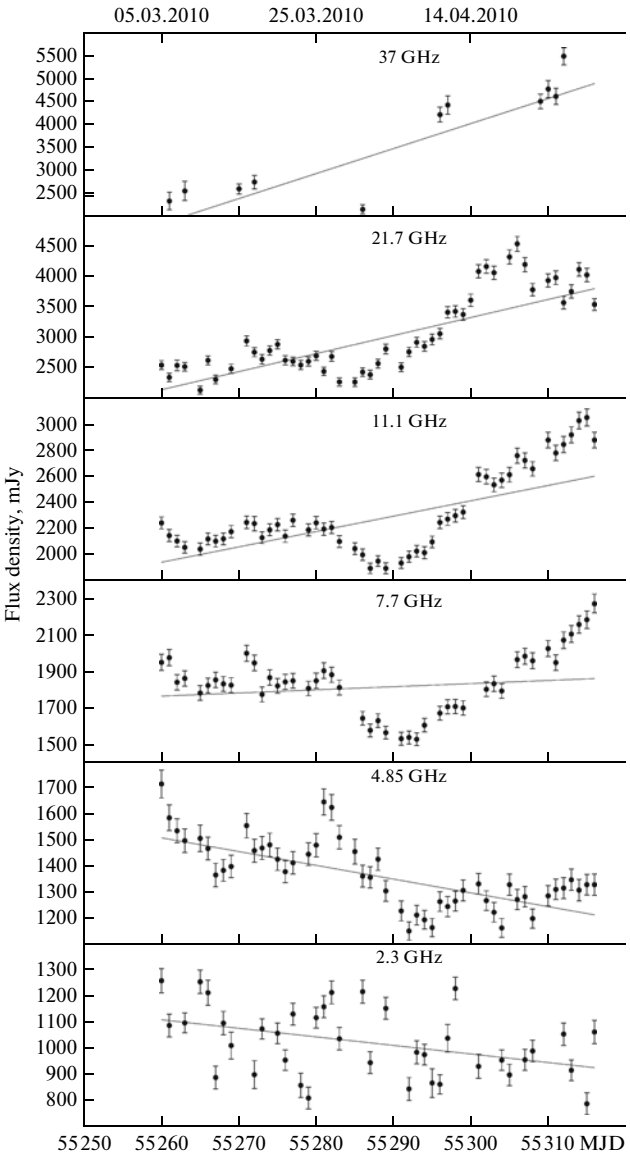

Fig. 1. Light curves of J0721+7120 at six radio frequencies (RATAN-600 and Metsähovi data).

3. SEARCH FOR VARIABILITY AND DETERMINATION OF ITS PARAMETERS

The search for variability on scales from several days to several weeks and study of the parameters of this variability based on the obtained series of observations were conducted in several stages.

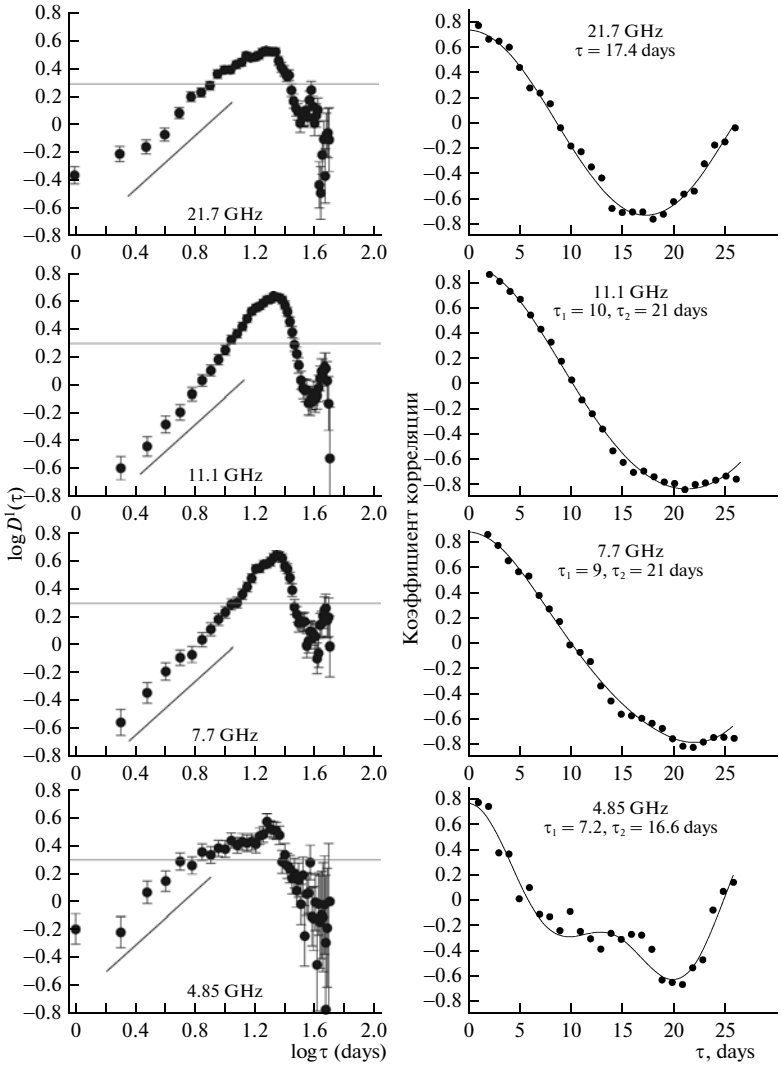

Fig. 2. First-order structure functions D^1 (left) and auto-correlation functions (right) of the light curves of J0721+7120 at the five RATAN-600 frequencies presented in Fig. 1.

First, we filtered out measured flux densities corrupted by any kind of interference (weather conditions or man-made interference) using the Fisher criterion. We assumed that all data records should belong to the same general population; therefore, we found the maximum number of records satisfying the Fisher criterion with a 1% significance level. In the subsequent analysis, we used only flux densities selected by the Fisher criterion in an entire cycle of measurements.

We then removed long-term variability with time scales longer than the duration of the observations. This variability appears as trends with various characters, which we approximated using a quadratic polynomial and eliminated from the initial records. We determined the mean flux density of the source at all the observed frequencies during an entire cycle of observations or in a selected time interval.

We then calculated the normalized χ^2 for a cycle (or part of a cycle) of observations for a number of degrees of freedom $n-1$, where n is the number of observations during the considered interval:

$$\chi^2 = (n-1)^{-1}\Sigma((S_i - \langle S\rangle)/\Delta S_i)^2,$$

where S_i and ΔS_i are the mean flux density for the ith observation of the considered time interval and its error, and $\langle S\rangle$ is the mean flux density in the considered interval.

We took variability to be detected if χ^2 exceeded the value for the 1% significance level for $n-1$ degrees of freedom in the RATAN-600 observations.

To determine the characteristics of the variability (the time scales and variances of the variable component), we calculated first-order structure functions

Table 1. Results of observations of J0721+7120 at 6.2 cm

Date	MJD	$\langle S\rangle$, mJy	ΔS, mJy	χ^2	$\chi^2(0.1\%)$	$N-1$	S_{var}, mJy	τ_{acf}, h
Mar. 19, 2010	55274.602	1474	4	3.25	2.97	10	25	
Mar. 20–21, 2010	55275.570	1443	8	28.61	2.52	15	104	8
Mar. 27–28, 2010	55283.285	1599	8	8.67	2.58	14	103	
Apr. 2–3, 2010	55289.348	1285	5	3.16	3.49	7	0	
Apr. 11, 2010	55297.633	1296	4	2.95	3.28	8	0	
Apr. 17–19, 2010	55304.133	1275	5	4.80	2.40	17	60	
May 9, 2010	55325.492	1464	12	44.40	2.75	12	157	
May 15–16, 2010	55332.297	1310	11	11.94	2.40	17	167	
May 22–23, 2010	55339.145	1291	9	21.76	2.75	12	84	10
June 13–14, 2010	55360.570	1466	7	32.73	2.52	15	100	13
July 29–30, 2010	55406.926	1445	17	26.68	2.66	13	158	
Aug. 31, 2010	55439.496	1324	4	8.60	2.66	13	50	12
Sep. 19–20, 2010	55459.258	1831	4	7.60	2.85	11	44	
Oct. 19–20, 2010	55488.980	1747	7	16.11	1.92	34	166	16

Table 2. Results of observations of J0721+7120 at 3.5 cm

Date	MJD	$\langle S\rangle$, mJy	ΔS, mJy	χ^2	$\chi^2(0.1\%)$	$N-1$	S_{var}, mJy	τ_{acf}, h
Apr. 15, 2010	55301.461	2020	83	307.29	3.77	6	448	5
Apr. 21, 2010	55307.426	2010	11	21.85	4.14	5	49	5
Apr. 29, 2010	55315.430	2239	10	12.13	4.14	5	45	
June 26–27, 2010	55374.086	1500	6	15.61	2.40	17	67	6

(SFs), auto-correlation functions (ACFs), and cross-correlation functions (CCFs). We used the SFs initially to determine the variance of the variable component:

$$\sigma^2_{var} = \sigma^2_{pr} - \sigma^2_n, \qquad (1)$$

where $\sigma^2_{pr} = \sum_{i=1}^{n}(S_i - \langle S\rangle)^2/(n-1)$ is the variance of the process, $\sigma^2_n = D^1(1)/2$ is the variance of the noise component, and $D^1(1)$ is the value of the SF shifted by one point.

We characterized the amplitude of the variable component by the modulation index, defined as $m = 100\sigma_{var}/\langle S\rangle$.

We used the shape of the SF to determine the variability time scales. Above the level of the instrumental noise, the SF grows according to a power law until it reaches a saturation level. The intersection of the power-law part with the saturation level also yields the time scale τ_{sf}.

Variability time scales τ_{acf} can be determined more accurately from the first minimum of the ACF. In this case, the time scale τ_{acf} for periodic (cyclic) flux-density variations is half of a period (cycle).

We also calculated CCFs between frequency channels in which variability was detected. The technique used to determine the time scales τ_{acf}, τ_{ccf}, and the time delays between frequency channels is described in [4].

The technique used to determine the parameters of the observed intraday variability is described in [10]. In our IDV study, we took variability to be detected if χ^2 exceeded the value for a significance level of 0.1%. This toughening of the requirements for the significance level for the observations on the 32-m antenna is connected with the larger number of parameters to be taken into account when determining the flux densities in each observing cycle. Since we could not construct SFs for all the cycles of the IDV observations, the flux density of the variable component

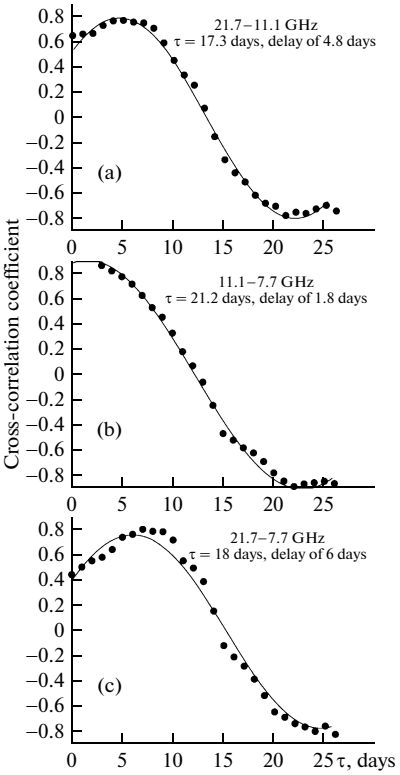

Fig. 3. Cross-correlation functions of the RATAN-600 light curves of J0721+7120 (Fig. 1) between 21.7 and 11.1 GHz, 11.1 and 7.7 GHz, and 21.7 and 7.7 GHz.

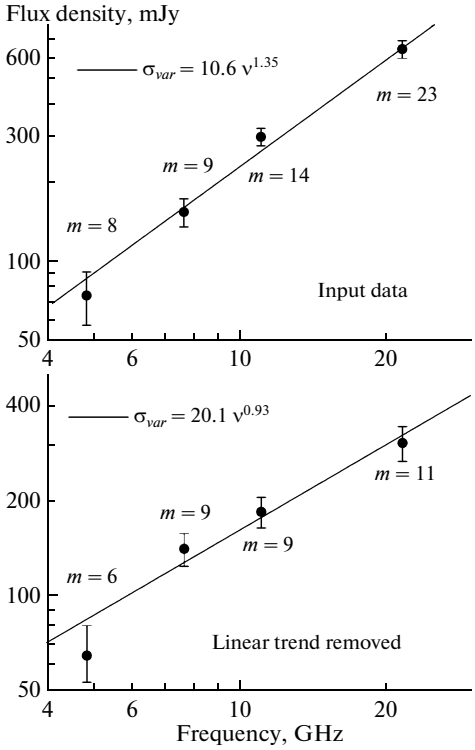

Fig. 4. Spectra of the flux-density standard of the variable component σ_{var}. Modulation indices m for each frequency are also given.

in a given observing cycle was determined using the following formula, taken from [11]:

$$S_{var} = [(n-1)(\chi^2 - 1)/\Sigma\Delta S_i^{-2}]^{0.5}.$$

4. RESULTS

4.1. Variability on Time Scales Longer than a Day

Figure 1 shows the RATAN-600 and Metsähovi light curves of J0721+7120 at six frequencies.

The variability of J0721+7120 is visible even by eye at all frequencies except for 2.3 GHz. At 37–7.7 GHz, the variability appears as an isolated flare, while it has a more complex character at 4.85 GHz. The maximum flux densities essentially coincide with those obtained for the entire time of monitoring of the source at 37–4.8 GHz since 1981 [3].

To study the amplitude–frequency characteristics of the variability, we constructed SFs, ACFs (Fig. 2), and CCFs (Fig. 3) for the entire set of RATAN-600 observations after removing a linear trend. The small number of observations and their irregularity hindered us from obtaining these functions at 37 GHz.

The line in the left-hand graphs of Fig. 2 shows the dependence $\mu = d\log D/d\log\tau = 1$, which describes the slope of the line connecting the top and bottom plateaus of the SF. The slope μ is determined by the power spectrum of the process $P(f)$; if $\mu = 1$, the variations have a shot-noise character and result from damped white-noise pulses with a restricted spectrum.

The SFs and ACFs indicate significant variability at 21.7–4.85 GHz and an absence of variability at 2.3 GHz. The exact values of τ_{acf} for each frequency were obtained from the ACFs using the technique described in [4]. The variation time scale at 21.7 GHz is $\tau_{acf} = 17$ d, with a modulation index $m = 11\%$. At 11.1 and 7.7 GHz, $\tau_{acf} = 21$ d, with the modulation indices $m = 9\%$ at both frequencies. A very weak variable component (with an amplitude approximately a factor of 15 smaller) with $\tau_{acf} = 9 - 10$ d was also detected at these frequencies. Two time scales, $\tau_{acf} = 7$ d and $\tau_{acf} = 17$ d, can be detected at 4.85 GHz, with the modulation index $m = 6\%$. The amplitude of the variability with the longer τ_{acf} is twice that of seven-day variability.

Since the 37-GHz data are not sufficient to construct the ACF, we determined the flare time scale using the technique proposed in [12]. In this case, the time scale is defined to be $\tau_{var} = dt/d\ln S$. Strictly speaking, this definition is correct only for exponential flares, and we used this only as an estimated time

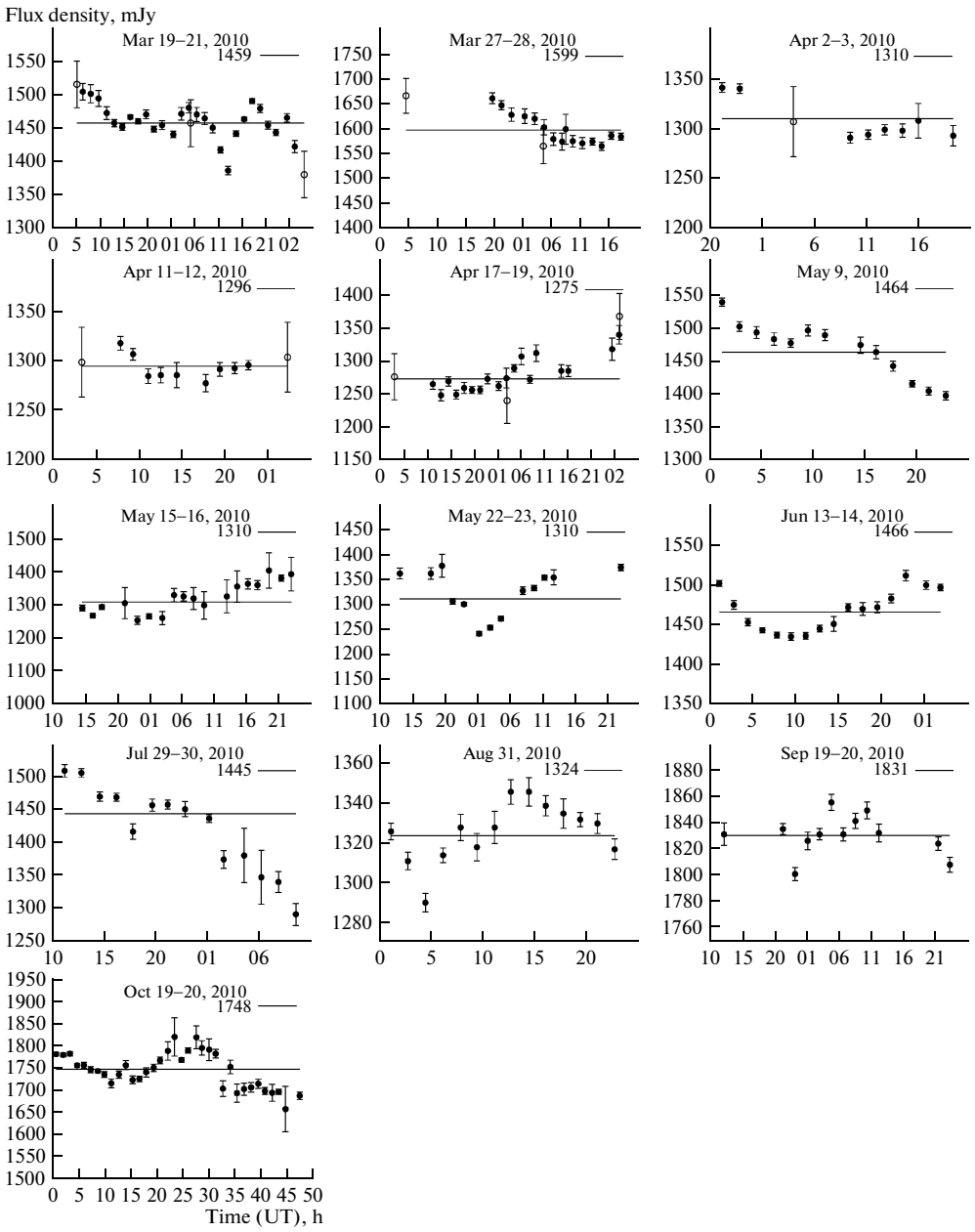

Fig. 5. Light curves of J0721+7120 during individual observing sessions at 6.2 cm (filled cicrles). Each point is the flux density averaged over the cycle. The open circles show the corresponding RATAN-600 data. The horizontal line shows the mean flux density for each session without the RATAN-600 data.

scale. Nevertheless, the resulting time scale $\tau_{var} =$ 20 d is in a good agreement with the values $\tau_{acf} =$ 17–21 d obtained at the other frequencies.

The CCFs enable us to determine time delays in the development of the variability between frequencies. The development of the variations at 11.1 GHz is delayed by 4.6 days compared to their development at 21.7 GHz (Fig. 3a). The process developed 1.6 days later at 7.7 GHz than at 11.1 GHz (Fig. 3b). The frequency ratios in the former and latter cases are 1.95 and 1.44; in view of the uncertainties, the delay as a function of frequency is probably close to linear or slightly decreasing with decreasing frequency. Figure 3c shows the CCF between 21.7 and 7.7 GHz, which indicates a delay of 6 days.

We were able to use formula (1) to determine σ^2_{var} at four frequencies for the longer time scale. The analysis of the SFs of the input data shows that the spectrum of the variable component σ_{var} is rising and fairly steep: $\sigma_{var} = 10.5\nu^{1.35}$ (Fig. 4a). The removal of a linear trend in the input data slightly reduces the slope of the spectrum of the variable component:

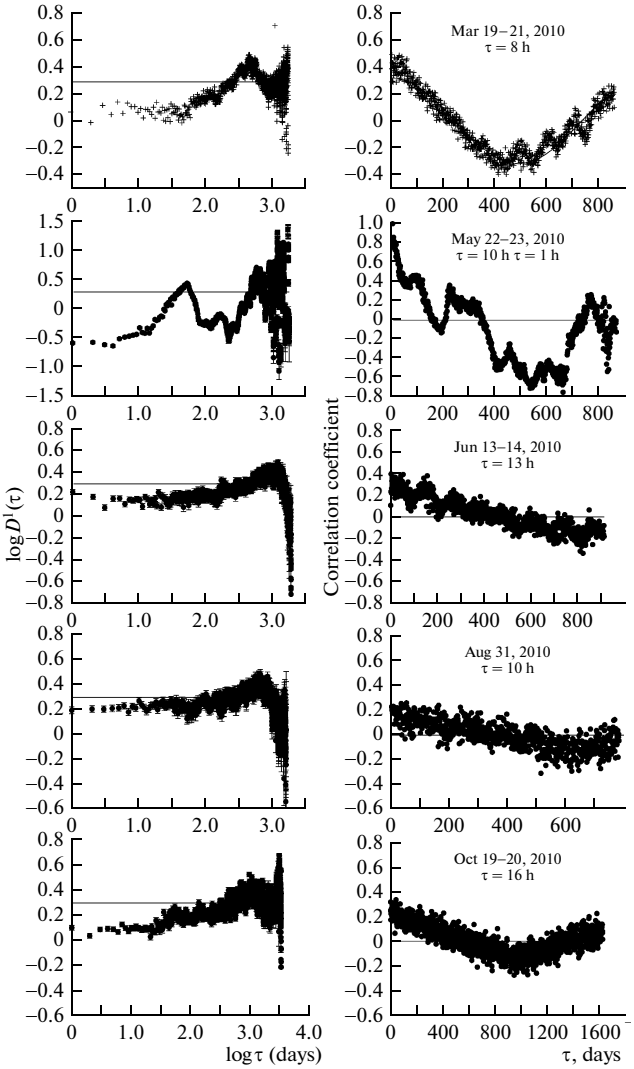

Fig. 6. Structure functions (left) and autocorrelation functions (right) for five observing sessions of J0721+7120 in which IDV was detected. The interval between the points is 59 s.

$\sigma_{var} = 20\nu^{0.93}$ (Fig. 4b). Figure 4 shows also the modulation indices for each frequency.

The spectrum of the variable component with a time scale of 7–10 days could not be determined due to its small amplitude. It is clear only that the flux density of the variable component with this time scale decreases toward higher frequencies.

4.2. Variability on Short Time Scales

We carried out 16 observing sessions at 6.2 cm and five sessions at 3.5 cm at the Zelenchukskaya Observatory up to October 19, 2010. The results of these observations are listed in Table 1 (6.2 cm) and Table 2 (3.5 cm). The columns of the tables give the (1) date of the observation, (2) Julian date (MJD) to which the (3) mean flux density is referred, (4) uncertainty in the mean flux density, (5), (6) normalized χ^2 for the actual observations and the theoretical value for the 1% significance level, (7) number of degrees of freedom, (8) flux density of the variable component, and (9) variability time scale τ_{acf} in hours obtained from the analysis of the ACFs. All flux densities are given in milliJansky.

The filled circles in Fig. 5 show the cycle-averaged flux densities for the 13 sessions at 6.2 cm. The data for March 19–21, April 17–19, and October 19–20 were combined into one session. The open circles in Fig. 5 show the RATAN-600 data obtained on these days at the same wavelength. Figure 5 also shows the flux densities averaged over a session without the RATAN-600 data.

Intraday variability was detected in five sessions: March 19–21, May 22–23, June 13–14, August 31, and October 19–20. Figure 6 presents the SFs and ACFs for these sessions. The time scale for the first

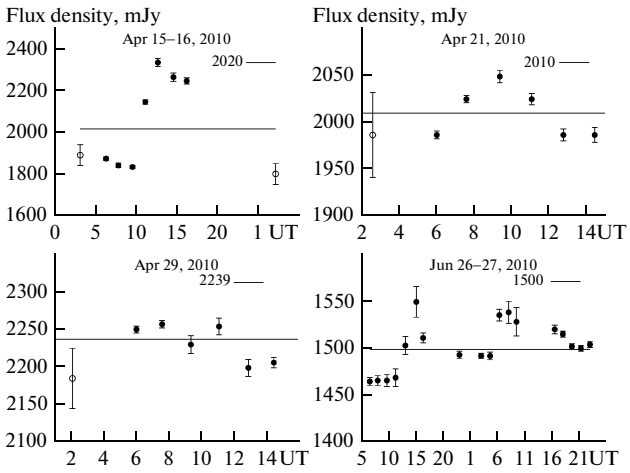

Fig. 7. Same as Fig. 5 for observations at 3.5 cm.

session found using the technique of [4] is $\tau_{acf} = 8$ h; the IDV flux density is $S_{var} = 104$ mJy. For the second session, $\tau_{acf} = 10$ h and $S_{var} = 84$ mJy. This session may also include faster variability with $\tau_{acf} = 1$ h. The remaining three sessions show IDV with time scales $\tau_{acf} = 13, 10, 16$ h and $S_{var} = 100, 50, 166$ mJy.

In two sessions, on April 2–3 and April 11–12, no variability was detected.

In the remaining sessions, variability appeared as trends on time scales longer than a day; this is a consequence of variability at 4.85 GHz with time scales longer than 7 d (see the light curve at 4.85 GHz in Fig. 1).

In Fig. 7, the mean flux densities for observations in five sessions at 3.5 cm are shown with filled circles; the open circles show the RATAN-600 data obtained on these days. Figure 7 also shows the mean flux densities for the sessions without the RATAN-600 data.

Variability was detected in all sessions. The most significant IDV was detected on April 15, with $S_{var} = 450$ mJy and $\tau_{sf} = 5$ h. In the session of April 21, IDV with $\tau_{acf} = 4.5$ h was present, but S_{var} was an order of magnitude lower than in the previous case. In the session of April 29, the observed variability was most likely a weak linear trend. In the session of June 26–27, there was IDV with $\tau_{acf} = 6$ h and $S_{var} = 75$ mJy.

5. CONCLUSIONS

(1) The delay in the development of the flare of 2010 between 21.7 and 7.7 GHz is the largest for all observed flares: six days. Based on this delay, we can estimate the Lorentz factor $\gamma = 34–38$. In the flares of 2004 and 2007, the delay was 3–3.5 days, implying $\gamma = 45–50$ [3].

(2) The angle θ between the line of sight and the jet is 2°.

(3) The group velocity $\beta = v/c$ is 0.99894 for $\beta_{app} = v_{app}/c = 20$.

(4) The brightness temperature T_b during the flare of 2010 is $(4–10) \times 10^{14}$ K at 21.7–7.7 GHz; this corresponds to the Doppler factor $\delta = 7–10$ based on the inverse-Compton limit.

(5) A more correct estimate, $\delta = 20$, can be made based on $\gamma = 35$ and $\theta = 2°$, within the limits obtained from the equipartition condition.

(6) The amplitude of the flare of 2010 is comparable to that of the powerful flare of 2004, but its time scale is a factor of five to eight shorter than for the flares of 2004 and 2008 [3]. Note that the flare was preceded by a decrease in the flux density relative to the mean level, as is characteristic of the majority of sources with flare activity. The flare took place approximately one year earlier than had been expected based on estimates of the precession of the system, $\geq$25 years. It is possible that the precession period in [3] was estimated incorrectly. The difference in the flare characteristics also admits the possibility that this flare is not related to the precession period and was a consequence of activity of the jet. Therefore, further monitoring of J0721+7120 in 2011–2012 is desirable.

(7) IDV is present in approximately one-third of the sessions at 6.2 cm with time scales $\tau_{acf} = 8–16$ h. A similar time scale, $\tau_{acf} = 11$ h, was observed in three of nine sessions in the active phase of the source in 2009 [4]; in the quiescent state of the source (four sessions), IDV was absent. IDV is related to the appearance of compact structures in the source and is most likely a consequence of interstellar scintillations.

ACKNOWLEDGMENTS

The authors are grateful to the Finnish Academy of Science and Letters for the support of the observational work at Metsähovi (grant nos. 212656, 210338, and 1211148). This work was also supported by the Russian Foundation for Basic Research (project code 10-02-00292-a).

REFERENCES

1. H. Kühr, A. Witzel, I. I. K. Pauliny-Toth, et al., Astron. Astrophys. Suppl. Ser. **45**, 367 (1981).
2. K. Nilsson, T. Pursimo, A. Sillanpää, et al., Astron. Astrophys. **487**, L29 (2008).
3. A. E. Vol'vach, M. G. Larionov, N. S. Kardashev, et al., Astron. Rep. **53**, 777 (2009).
4. A. G. Gorshkov, A. V. Ipatov, V. K. Konnikova, et al., Astron. Rep. **55**, 97 (2011).
5. G. Tagliaferri, M. Ravasio, G. Ghisellini, et al., Astron. Astrophys. **400**, 477 (2003).
6. L. Furman, T. P. Krichbaum, A. Witzel, et al., Astron. Astrophys. **490**, 1019 (2008).
7. A. G. Gorshkov, V. K. Konnikova, and M. G. Mingaliev, Astron. Rep. **47**, 903 (2003).
8. A. G. Gorshkov and O. I. Khromov, Izv. Spets. Astrofiz. Observ. **14**, 15 (1981).
9. D. V. Ivanov, A. V. Ipatov, I. A. Ipatova, et al., Tr. Inst. Prikl. Astron. **12**, 93 (2005).
10. A. G. Gorshkov, A. V. Ipatov, I. A. Ipatova, et al., Astron. Rep. **53**, 389 (2009).
11. G. A. Seielstad, T. J. Pearson, and A. C. S. Readhead, Publ. Astron. Soc. Pacif. **95**, 842 (1983).
12. E. Valtaoja, A. Lähteemäki, H. Teräsranta, and M. Lainela, Astrophys. J. Suppl. Ser. **120**, 95 (1999).

Translated by G. Rudnitskii